# Co-Optimizing Substation Hardening and Transmission Expansion Against Earthquakes: A Decision-Dependent Probability Approach

Diego Alvarado, Rodrigo Moreno, *Member, IEEE*, Alexandre Street, *Member, IEEE*, Mathaios Panteli, *Senior Member, IEEE*, Pierluigi Mancarella, *Senior Member, IEEE*, and Goran Strbac, *Member, IEEE*

***Abstract*—In light of the rising frequency and impact of natural hazards on power systems, planning resilient network investments is becoming increasingly important. This task, however, needs, in addition to widely accepted investment options focused on installing new infrastructure, explicit recognition of investment propositions to harden existing infrastructure such as substations. Hardening networks is fundamentally challenging to incorporate in optimization problems since it affects outage probabilities. Therefore, we propose an optimization approach to determine optimal portfolios of resilient network investments, considering endogenous probabilities that change with hardening investment options. This decision-dependent-probability model finds the optimal network enhancements in a cost-benefit fashion, minimizing investment plus operational costs, including demand curtailments. The proposed model also considers distributed energy resources (DER), which can displace costly network investments. Additionally, the model takes into account the lack of fully accurate fragility curves; thus, outage probabilities are not only affected by hardening decisions but also by the inherent uncertainty associated with fragility modeling. This is a key concern in practical resilience assessment and is addressed in this work through a global-convergent exact algorithm. Case studies applied on earthquakes in Chile demonstrate the benefits of our proposed network planning approach.**

***Index Terms*—Decision dependent probability, power systems economics, power system resilience, transmission expansion planning.**

Manuscript received 30 June 2021; revised 5 January 2022 and 13 April 2022; accepted 21 May 2022. Date of publication 9 June 2022; date of current version 24 April 2023. The work of Alexandre Street was supported in part by Conselho Nacional de Desenvolvimento Científico e Tecnológico (CNPq) and in part by Fundaçao de Amparo à Pesquisa do Estado do Rio de Janeiro (FAPERJ). This work was supported in part by ANID, Chile, under Grants PIA/APOYO AFB180003 (Instituto Sistemas Complejos de Ingenieria) and Fondecyt /1181928, in part by Newton Fund through the Newton Prize under Grant MR/N026721/1, in part by Engineering and Physical Sciences Research Council (EPSRC) through Projects TERSE under Grant EP/R030294/1, and Disaster management and resilience in electric power systems under Grant EP/N034899/1, and in part by U.K. EPSRC Project: Technology Transformation to Support Flexible and Resilient Local Energy Systems under Grant EP/T021780/1. Paper no. TPWRS-01037-2021. *(Corresponding author: Rodrigo Moreno.)*

Diego Alvarado is with the Instituto Sistemas Complejos de Ingeniería, 1025000 Santiago, Chile (e-mail: d.alvarado@isci.cl).

Rodrigo Moreno is with Electrical Engineering, University of Chile, 1025000 Santiago, Chile, and with the Instituto Sistemas Complejos de Ingeniería, 1025000 Santiago, Chile, and also with the Imperial College London, SW7 2AZ London, Great Britain (e-mail: rmorenovieyra@ing.uchile.cl).

Alexandre Street is with the Laboratory of Applied Mathematical Programming and Statistics, and the Department of Electrical Engineering of the Pontifical Catholic University of Rio de Janeiro, Rio de Janeiro, Brazil (e-mail: street@ele.puc-rio.br).

Mathaios Panteli is with the Electrical and Computer Engineerng, University of Cyprus, 1678 Nicosia, Cyprus (e-mail: panteli.mathaios@ucy.ac.cy).

Pierluigi Mancarella is with the University of Melbourne, Department of Electrical and Electronic Engineering, 3010 VIC, Australia, and with the University of Manchester, Department of EEE, M13 9PL Manchester, UK (e-mail: pierluigi.mancarella@unimelb.edu.au, p.mancarella@manchester.ac.uk).

Goran Strbac is with the Imperial College, Electrical Engineering, SW7 2AZ London, United Kingdom of Great Britain and Northern Ireland (e-mail: g.strbac@imperial.ac.uk).

Color versions of one or more figures in this article are available at https://doi.org/10.1109/TPWRS.2022.3180363.

Digital Object Identifier 10.1109/TPWRS.2022.3180363

## NOMENCLATURE

*Functions*

| | |
|---|---|
| $\boldsymbol{y}(\cdot)$ | Function that determines corrective actions given pre-contingency decisions and contingency states. |
| $\mathcal{M}(\cdot)$ | Function that returns the set of all probability distributions with a given support. |
| $\mathcal{P}_{ts}(\cdot)$ | Function that returns the set of all outage probability distributions at time $t$ and scenario $s$, given the vector of hardening decisions. |
| $fr(\cdot)$ | Function that returns the index of the originating/sending substation of a given line. |
| $H_t(\cdot)$ | Function that computes the cost of corrective actions at time $t$, given the contingency and pre-contingency decisions. |
| $to(\cdot)$ | Function that returns the index of the receiving substation of a given line. |

*Sets*

| | |
|---|---|
| $\mathcal{A}$ | Set of system contingencies. |
| $\mathcal{D}$ | Set of indexes of substation damage states. |
| $\mathcal{E}$ | Set of indexes of power imbalance steps. |
| $\mathcal{I}$ | Set of indexes of all generators. |
| $\mathcal{I}_b$ | Set of indexes of generators connected to bus $b$. |
| $\mathcal{K}$ | Set of indexes of post-contingency snapshots. |
| $\mathcal{L}$ | Set of indexes of all transmission lines. |
| $\mathcal{L}^C$ | Set of indexes of candidate transmission lines. |
| $\mathcal{L}^E$ | Set of indexes of existing transmission lines. |
| $\mathcal{N}$ | Set of indexes of all substations. |
| $\mathcal{N}_h$ | Set of indexes of substations that can be hardened. |
| $\mathcal{S}$ | Set of indexes of scenarios. |

$\mathcal{T}$ Set of indexes of time blocks.
$\mathcal{W}$ Set of indexes of renewable generators.

*Parameters*

$\Delta t$ Total duration of each post-contingency snapshot.
$\delta$ Energy payback factor for the load shifting service.
$\mathbb{p}_s$ Probability of scenario $s$.
$\overline{\boldsymbol{\mu}}_{ts}$ Auxiliary vector used to construct first-order moment constraints for time block $t$ and scenario $s$.
$\overline{\Delta D}^{+}_{be}$ Maximum net load increase in substation $b$ and step $e$.
$\overline{\Delta D}^{-}_{be}$ Maximum net load reduction in substation $b$ and step $e$.
$\overline{\Delta}^{FD}_{b}$ Maximum demand shifting service in substation $b$.
$\overline{D}_b$ Maximum demand for substation $b$.
$\overline{F}_l$ Maximum flow through line $l$.
$\overline{P}_i$ Maximum power of generator $i$.
$\overline{R}^{D}_{ik}$ Maximum downward reserve of generator $i$ for snapshot $k$.
$\overline{R}^{U}_{ik}$ Maximum upward reserve of generator $i$ for snapshot $k$.
$\sigma^{N}_{m}$ Weight for the $m$th damage state of substations that determines capacity degradation.
$\underline{P}_i$ Minimum stable generation for generator $i$.
$\zeta_{wt}$ Availability of renewable generator $w$ at time block $t$.
$b_l$ Susceptance of line $l$.
$C^{d}_{ik}$ Scheduling cost of downward reserves for generator $i$ and snapshot $k$.
$C^{h}_{b}$ Cost of hardening substation $b$.
$C^{L}_{l}$ Investment cost of candidate line $l$.
$C^{p}_{i}$ Energy cost of generator $i$.
$C^{u}_{ik}$ Scheduling cost of upward reserves for generator $i$ and snapshot $k$.
$C^{dc}_{ik}$ Utilization cost of downward reserves for generator $i$ and snapshot $k$.
$C^{D}_{b}$ Demand curtailment cost for substation $b$.
$C^{FD^c}_{b}$ Utilization cost of the load shifting service on substation $b$.
$C^{FD}_{b}$ Cost of scheduling the load shifting service on substation $b$.
$C^{G}_{i}$ Generation curtailment cost for generator $i$.
$C^{I+^c}_{be}$ Utilization cost of the net load increase service on substation $b$ for step $e$.
$C^{I+}_{be}$ Cost of scheduling the net load increase service on substation $b$ and step $e$.
$C^{I-^c}_{be}$ Utilization cost of the net load reduction service on substation $b$ for step $e$.
$C^{I-}_{be}$ Cost of scheduling the net load reduction service on substation $b$ and step $e$.
$C^{uc}_{ik}$ Utilization cost of upward reserves for generator $i$ and snapshot $k$.
$D_{bt}$ Demand on substation $b$ at time bock $t$.
$h_t$ Number of hours represented by time block $t$.
$K_{ts}$ Matrix that modifies the probability distribution based on hardening decisions for time block $t$ and scenario $s$.
$M$ Large constant.
$S_{ts}$ Auxiliary matrix used to construct first-order moment constraints for time block $t$ and scenario $s$.

*Decision Variables*

$\boldsymbol{a}_{ts}$ Binary vector containing availability and damage states of all system components at time block $t$ and scenario $s$.
$\boldsymbol{x}^{H}$ Vector of all hardening decisions.
$\boldsymbol{x}^{L}$ Vector of all investment decisions in new lines.
$\boldsymbol{x}^{Op}_{t}$ Vector of all operation continuous variables at time block $t$.
$\boldsymbol{x}^{UC}_{t}$ Vector of all unit commitment binary decision variables at time block $t$.
$\Delta D^{+}_{bet}$ Net load increase service scheduled on substation $b$ on step $e$ and at time block $t$.
$\Delta D^{-}_{bet}$ Net load reduction service scheduled on substation $b$ on step $e$ and at time block $t$.
$\Delta^{FD}_{bt}$ Load shifting scheduled on substation $b$ at time block $t$.
$\theta^{c}_{bk}$ Voltage angle of substation $b$ on snapshot $k$.
$\theta_{bt}$ Voltage angle of substation $b$ at time block $t$.
$a^{G}_{i}$ Binary variable that is equal to 0 if generator $i$ is unavailable, being 0 otherwise.
$a^{L}_{l}$ Binary variable that is equal to 0 if line $l$ is unavailable, being 0 otherwise.
$a^{N_m}_{b}$ Binary variable that is equal to 0 if substation $b$ is undergoing the $m$th damage state or worse, being 0 otherwise.
$d^{N}_{b}$ Fraction of the capacity of substation $b$ that remains available.
$f^{c}_{lk}$ Flow through line $l$ on snapshot $k$.
$p^{c}_{ik}$ Power output of generator $i$ on snapshot $k$.
$GS_{ik}$ Generation curtailment of generator $i$ on snapshot $k$.
$LS_{bk}$ Load shedding on substation $b$ on snapshot $k$.
$p^{c}_{ik}$ Power output of generator $i$ on snapshot $k$.
$p_{it}$ Power output of generator $i$ at time block $t$.
$r^{d}_{ikt}$ Downward reserves scheduled on generator $i$ for snapshot $k$ at time block $t$.
$r^{u}_{ikt}$ Upward reserves scheduled on generator $i$ for snapshot $k$ at time block $t$.
$r^{dc}_{ik}$ Downward reserves delivered by generator $i$ on snapshot $k$.
$r^{uc}_{ik}$ Upward reserves delivered by generator $i$ on snapshot $k$.
$x^{H}_{b}$ Binary investment decision to harden substation $b$.
$x^{L}_{l}$ Binary investment decision for candidate line $l$.
$x^{UC}_{it}$ Commitment status of generator $i$ at time block $t$.
$\Delta^{FD+c}_{bk}$ Positive deviation from nominal demand on substation $b$ due to load shifting on snapshot $k$.
$\Delta^{FD-c}_{bk}$ Negative deviation from nominal demand on substation $b$ due to load shifting on snapshot $k$.
$\Delta D^{+c}_{bke}$ Net load increase on substation $b$ on snapshot $k$ for step $e$.
$\Delta D^{-c}_{bke}$ Net load reduction on substation $b$ on snapshot $k$ for step $e$.

# I. Introduction

## A. Motivation

NATURAL hazards threaten the integrity of power systems across the globe, with catastrophic consequences to the electricity consumers and the overall society. To protect power systems against natural hazards such as earthquakes, tsunamis, and hurricanes, a richer set of investment options must be used to effectively enhance system resilience, going beyond those traditionally considered in transmission expansion planning problems [1]. Indeed, while the economic and reliability performance of power networks have been classically improved by expanding the network (installing more network infrastructure), resilience can also be tackled by hardening existing infrastructure as indicated in [1] and [2]. Examples of hardening decisions include undergrounding lines to deal with high wind speeds [3], upgrading poles with stronger, more robust materials [3], building substation defenses to deal with flooding events [4], and anchoring substation equipment to better deal with earthquakes [1]. In this paper, we focus on applications on earthquakes since they represent one of the major threats to power systems [5].

In case of seismic hazards, substation outages pose an important risk to the continuity of supply, as noted by [6] in the context of the 8.8Mw-magnitude earthquake that struck Chile in 2010. Therefore, in order to design transmission networks that are resilient against earthquakes, it is of great importance to consider substation hardening along with traditional investment alternatives focused on transmission expansion (i.e., new lines and transformers). Such hardening decisions feature the effect of decreasing failure probabilities conditional to an earthquake, which are calculated by using the so-called fragility curves. These curves provide a straightforward relation between the intensity of the hazard and the failure probability as indicated in [7]. As hardening decisions modify failure probabilities, stochastic programs become nonlinear and, therefore, more challenging and harder to solve. Traditionally, stochastic programs used in transmission investment planning assume probabilities as a set of (constant) parameters, and are thus not able to deal with hardening decisions.

Another key challenge in resilient network design is that failure probabilities calculated through fragility curves may present large errors, as these curves are elaborated under assumptions that may not apply in practice. Yet, these are widely used. For example, there is a diversity of assets' responses to hazards, which can greatly vary due to real characteristics that are not captured by fragility modeling [8]. Hence, due to the impact that such errors may have in reality, mathematical programs should prioritize investment plans that are immune, or robust, against imprecise fragility curves.

To appropriately tackle these challenges, network planning models that aim to enhance resilience against earthquakes must consider two key elements. Firstly, they need to also include, apart from investment decisions in network expansion, substation hardening decisions by introducing decision-dependent probabilities (endogenous probabilities). Secondly, to obtain a resilient plan, such models should acknowledge that fragility data (and fragility curves) are not fully reliable and that, in practice, decisions should hedge investment plans against these uncertainties too.

## B. Literature Review and Contributions

Resilient network design models aim to either enhance resilience against natural hazards (e.g., earthquakes, storms) [1], [9]–[17] or man-kind hazards (e.g., terrorist attacks) [18], [19]. In both cases, hardening decisions represent an effective measure to hedge against such threats. In this vein, an increasing body of work has considered hardening decisions within network investment planning models [1], [9]–[12], [14]–[17], [20]–[22]. However, only a few works have proposed models that truly recognize the decision-dependent nature of failure probabilities. The latter fall into the class of optimization problems with decision-dependent uncertainty, as they are mathematical programs designed under the assumption that uncertainties are endogenous, dependent on the decisions being optimized.

In [14], [15], line hardening is co-optimized with investments in new infrastructure to enhance the resilience of distribution systems. The optimal investment portfolio is obtained by optimizing against a set of scenarios in a sample average approximation fashion, where the availability of candidate lines is sampled using different failure probabilities. Reference [9] also studies the hardening of distribution lines for resilience enhancement, modeling the failure of system components along with the post-disaster restoration process. The authors propose a robust reformulation to obtain an approximate solution, circumventing the problem of decision-dependent probabilities. The model proposed in [16] determines the optimal portfolio of resilient network investments, including transmission line construction and hardening, where the latter is modeled considering decision-dependent probabilities. The proposed approach aims to identify the portfolio that minimizes the impact of extreme weather events while satisfying budget constraints. Although this is practical, notice that the resilience level is determined by the prescribed budget rather than by a cost-benefit balance.

Hardening substations has been recognized as critical to face natural disasters such as earthquakes. Ideally, the expenditure in hardening measures should be co-optimized with others that can enhance resilience too, for example, investments in new lines [1]. Both new lines and hardening substations have been proved effective to deal with earthquakes. To the best of our knowledge, this problem has only been addressed in [1], [23], where the complexities associated with decisions-dependent probabilities are not explicitly modeled as the problem is solved through a "black-box" heuristic approach, namely, optimization via simulation. Therefore, no model has been proposed in the literature so far that can provide an exact solution for this network planning problem. Another disadvantage of the existing formulation is that it resorts to an exogenous budget constraint to select the portfolio that minimizes expected costs. From a cost-benefit viewpoint, though, the expenditure to enhance resilience should be a result of the optimization model rather than an input.

In this context, we propose an optimization model that identifies optimal portfolios of resilient network enhancements

against earthquakes from an economic, cost-benefit perspective. In order to hedge the system against earthquakes, we model two investment alternatives, namely, the construction/expansion of new transmission lines and substation hardening. Remarkably, we utilize an adjusted distributionally robust optimization (DRO) framework capable of dealing with decision-dependent probabilities straightforwardly. Furthermore, leveraging the DRO nature of the proposed model, we can readily capture how investment decisions are affected by imprecise outage probabilities derived from inaccurate fragility curves. We summarize the contributions of this work as follows:

1) A new resilient network investment model capable of co-optimizing substation hardenings with transmission expansions to protect the system against earthquakes. We do so by modeling hardening decisions through endogenous probabilities, which allows us to capture the value of these decisions within the optimal network investment plan.
2) Address the problem of imprecise fragility curves. Based on this model, we are able to plan investments that are robust against natural hazards under incomplete information about failure probabilities conditional to earthquakes.
3) Consider a more complete reliability model in terms of failure states that includes failures of substation equipment. By doing so, we are able to better represent the true post-contingency state of the system after a natural hazard occurs and thus capture the value of substation hardening.
4) Demonstrate that the portfolio of network investments (including hardening existing assets) can be efficiently complemented with DER services to enhance the resilience of the system and also hedge it against imprecise (or, using the terminology of DRO, ambiguous) fragility data.

Finally, note that although we illustrate the proposed modeling framework on earthquakes, this can be applied to other hazards.

### C. Paper Structure

This paper is structured as follows. Section II presents the modeling framework to determine resilient network enhancements and Section III discusses the algorithms to solve the problem. Sections IV and V present the case studies, their results, and the discussions. Finally, Section VI concludes.

## II. The Resilient Planning Model

### A. Overview

The proposed model determines the optimal portfolio of resilient network investments, considering decision-dependent probabilities of outage scenarios. The model belongs to the class of two-stage stochastic optimization models with endogenous probabilities. While investment in new infrastructure (lines and transformers) and also hardening decisions are made in a first stage (i.e., before the realization of contingencies/outages), post-contingency corrective dispatch actions are considered in the second stage (i.e., scenario-dependent decisions). The uncertainty scenarios are represented by binary vectors comprising generation and network statuses. Of utmost importance, hardening network infrastructure changes the value of outage probabilities, which is fundamentally challenging and complex to be considered in classical two-stage stochastic programming models. The challenge of considering decision-dependent probabilities is addressed in our work by using a DRO framework with first-moment constraints that are adjusted by hardening decisions. As shown in our case study section, this significantly changes the way natural hazard can be tackled by system planners.

Moreover, as an attempt to reduce network investments, we model three services from DER, namely, net load reductions (which can be achieved by voluntary demand curtailments and/or increasing distributed generation outputs), net load increases (which can be achieved by voluntarily increasing demand levels and/or distributed generation curtailments), and demand shifting. A detailed discussion about how DER can contribute to security of supply at the main system level (including detailed modeling aspects) is presented in [24]–[28].

The model minimizes investment and operational costs over a target year, which is represented by several time slices or time blocks. Although these blocks are time-decoupled, each of them, in turn, is divided into several post-contingency snapshots that are time-coupled so as to appropriately capture the evolution of the post-contingency operation in each scenario. The operational costs include the cost of network operation during the intact system (i.e., pre-contingency) as well as the expected costs of post-contingency operational decisions.

When analyzing resilience, a higher number of assumptions, involving the so-called fragility curves, are made to determine the ultimate probability values of network failures. Therefore, we take advantage of the DRO nature of our proposed model to analyze the effects of considering inaccurate (i.e., partially known) outage probabilities. The common approach to calculate these probabilities from fragility curves is maintained and used in our approach to provide referential values from which the actual failure probabilities deviate. In this way, the proposed model can readily address the lack of high-quality reliability and fragility data, which is a challenge in every probabilistic approach to planning network infrastructure aiming to enhance reliability and resilience.

### B. The Uncertainty and Decision-Dependent Probabilities

*1) The Scenario Tree:* Fig. 1 depicts the scenario tree used in our model and also illustrates the sequence of decisions and events considered, which we describe next:

1) Decisions related to network enhancements (regarding investment in new lines, $\boldsymbol{x}^L$, and substation hardening, $\boldsymbol{x}^H$) are determined, along with pre-contingency operation decisions (unit commitment, $\boldsymbol{x}^{UC}$, and operating points variables, $\boldsymbol{x}^{Op}$) for each time block, $t$, that represents $h_t$ hours of the target year.
2) The system undergoes a set of earthquake scenarios, where each scenario, $s$, is associated with a probability $\mathbb{p}_s$.
3) Under each earthquake scenario the system undergoes a set of contingencies (described by the state vector $\boldsymbol{a}$), whose conditional probabilities are dependent on both the

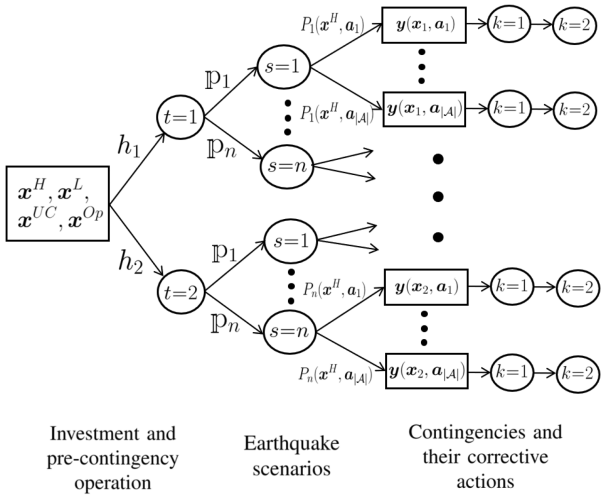


Fig. 1. Scenario tree of the problem.

earthquake scenario and hardening investment decisions made in the first stage.

4) Recourse corrective actions are determined for every post-contingency snapshot, $k$, in the vector $\boldsymbol{y}(\cdot)$ as a function of first-stage decisions and contingency states.

*2) Threat Characterization and Earthquake Scenarios:* Based on historical data, we select a sample of earthquakes with given magnitudes and locations. For each earthquake, we calculate its (spatial) attenuation profile by using the model proposed by Boroschek [29]. This is applied to calculate the peak ground acceleration (PGA) at the position of each network equipment as in [1].

*3) Vulnerability Assessment and Outage Probabilities:* The outage probabilities of system components, conditional to the occurrence of an earthquake, are calculated through fragility curves which are a function of the PGA at the location of every system equipment as in [1]. We use the fragility curves specified in [7], [30] for transmission line towers, generating units and substations. We compute the failure rate of transmission lines by assuming that every line is composed of several towers distanced by 300 meters, and that the line fails when any of its towers fails. This captures the fact that longer transmission lines are more vulnerable to earthquakes than shorter lines. Also, transmission lines can be affected due to failures in one of their substations. In the case of HVDC links, we use the same fragility model related to towers and substations as in the AC case. Nevertheless, it is possible to use a different set of fragility curves to model substations with converter equipment. The shape and special treatment of fragility curves within our resilient planning optimization model are explained next.

*4) Decision-Dependent Probabilities Via DRO:* In order to model decision-dependent probabilities, we optimize against the worst-case probability distribution within a set that is adjusted by hardening decisions, $\boldsymbol{x}^H$. As we explain next, the proposed methodology allows us to impose linear constraints over the outage probability of components (including partial outages for substations), thereby being able to make them equal to values that change with hardening decisions. Additionally, we can model inaccurate outage probabilities by using intervals (that also change with hardening decisions) instead of precise values, letting the problem choose the array of probabilities that maximize expected cost. To do so, we consider that the set of candidate probability distributions of outage events following an earthquake scenario $s$, in time block $t$, has the structure presented in (1).

$$\mathcal{P}_{ts}(\boldsymbol{x}^H)=\left\{P \in \mathcal{M}_+(\mathcal{A}) : \mathbb{E}_P[S_{ts}\boldsymbol{a}_{ts}] \leq \overline{\boldsymbol{\mu}}_{ts} + K_{ts}\boldsymbol{x}^H\right\}. \quad (1)$$

In (1), $\mathcal{M}_+(\mathcal{A})$ is the set of probability distributions with support on $\mathcal{A}$. $S_{ts}$ and $\overline{\boldsymbol{\mu}}_{ts}$ are used to construct general first-order moment constraints. $K_{ts}$ is the matrix that contains the information about changes in the probabilities prompted by hardening decisions. The random binary vector $\boldsymbol{a}_{ts}$ represents the state of system components in every time block $t$ and scenario $s$. It contains one element for each generator and transmission line, being equal to one if the corresponding component is available and zero otherwise. In addition, it contains one element for each damage state of each substation, which are ordered in increasing severity. These are used to model intermediate failures leading to partially available capacities of substations, whose relevance is explained in [1], [7]. We consider that a substation is operating normally when all its associated element in $\boldsymbol{a}_{ts}$ are equal to one. On the other hand, the $m$th damage state is represented by the first $m$ elements being equal to zero and the rest equal to one. In order to avoid infeasible states, we impose that the element associated with a given damage state can be zero only if all the previous elements (i.e., those associated with less severe damage states) are zero.

Note that a set of linear inequalities on the expected value of the elements of $\boldsymbol{a}_{ts}$ is used to construct the set of probability distributions in (1). Interestingly, since the availability is a Bernoulli random variable, its expected value is exactly one minus the failure probability, which we utilize to constrain the failure rate of generators and transmission lines. This is a key modeling aspect that extends the ambiguity set proposed in [31] to consider decision-dependent probabilities. In the case of substations, the expected value of the element of $\boldsymbol{a}_{ts}$ associated with a given damage state is equal to one minus the probability of undergoing at least that level of damage. Therefore, we can also use the linear inequalities in (1) to modify the probability of substation partial outages.

Additionally, the support set $\mathcal{A}$ contains all contingencies that are considered in the model, comprising failures of generators, network components, and different partial damage states of substations. Hence, if we want to model up to $k$ simultaneous outages, $\mathcal{A}$ should be the set presented in (2).

$$\mathcal{A} = \Big\{(\boldsymbol{a^G}, \boldsymbol{a^L}, \boldsymbol{a^N}) \in \{0,1\}^{|I|+|\mathcal{L}|+|N|\cdot|\mathcal{D}|} : \sum_{i\in I} a_i^G + \sum_{l\in\mathcal{L}} a_l^L + \sum_{b\in N} a_b^{N_1} \geq |I| + |\mathcal{L}| + |N| - k, \; a_b^{N_m} \geq a_b^{N_{m-1}} \forall b \in N, m \in \mathcal{D} \setminus \{1\}\Big\}, \quad (2)$$

where $I$, $\mathcal{L}$, $N$ are the sets of indices related to generators, transmission lines, and substations, respectively. The set $\mathcal{D}$ contains the indices related to damage states of substations.

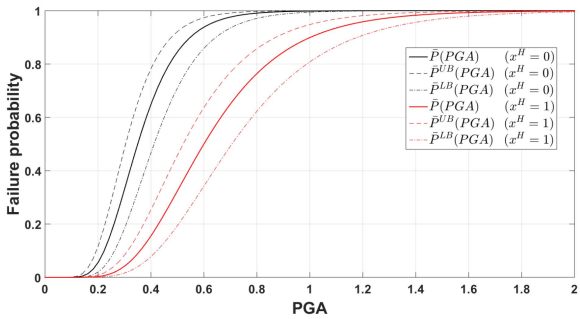


Fig. 2. Example of a fragility curve, its version for hardened components, and bounds used to model inaccuracies.

It is important to notice that the user can select any set of contingencies as the support $\mathcal{A}$. For example, the user may be interested in considering higher-order contingencies in certain regions of the system, which must be stated in the definition of $\mathcal{A}$.

Each damage state is associated with a fraction of the substation capacity that remains available, $d_b^N$. This fraction can be computed as the weighted sum of the binary variables $a_b^{N_m}$ as shown in (3). The weights $\sigma_m^N$ have to be properly selected, so the result of the sum is the targeted availability level.

$$d_b^N = \sum_{m\in\mathcal{D}} \sigma_m^N \cdot a_b^{N_m} \forall b \in N \tag{3}$$

Auxiliary matrix $S_{ts}$ and vector $\overline{\mu}_{ts}$ are selected so as to set the failure rate of each generator and line to its desired value, as well as the probability of substations' partial outages. Note that this requires two inequalities for each component of $\boldsymbol{a}_{ts}$, whose expected value must be set. The first one states that such expected value is less than or equal to the desired availability (i.e., $\mathbb{E}(a_{tsi}) \leq 1-\lambda_i^*$, where $\lambda_i^*$ is the desired outage rate), whereas the second one states that this expected value is greater than or equal to the desired availability (i.e., $\mathbb{E}(a_{tsi}) \geq 1-\lambda_i^*$). Note, however, that (1) considers only "less than or equal to" inequalities, so the second inequality is multiplied by minus one to comply with such requirement. In this way, $\overline{\mu}_{ts}$ must group the availability rates computed from fragility curves (except the sign in some elements), and the coefficients $K_{ts}$ must be selected so the desired availability is modified in both constraints when a substation is hardened, i.e., when the associated element of $\boldsymbol{x}^H$ is equal to one. In the hardened case, fragility curves are shifted to the right, as illustrated in the solid lines of Fig. 2, lowering the outage probabilities given a particular PGA value. In reference [7], fragility curves of hardened and normal substations are described.

When we consider inaccuracies in fragility curves, $S_{ts}$ and $\overline{\mu}_{ts}$ are selected in a way that the outage probability of each component lies within an interval, while also setting an upper bound to the sum of all outage probabilities, as in [24]. These intervals are computed utilizing upper- and lower-bound fragility curves, which can be constructed assuming a certain percentage of uncertainty. Examples of these curves are presented in Fig. 2, where a 15% uncertainty is considered in terms of PGA. This means that if substation $b$ undergoes a peak ground acceleration $PGA_{bts}$ on the time block $t$ of scenario $s$, its failure probability according to the nominal fragility curve would be $\bar{P}(PGA_{bts})$, the probability $\bar{P}^{LB}(PGA_{bts}) = \bar{P}(PGA_{bts}\cdot(1-0.15))$ would correspond to the lower bound, and $\bar{P}^{UB}(PGA_{bts}) = \bar{P}(PGA_{bts}\cdot(1+0.15))$ to the upper bound. The coefficients $K_{ts}$ are selected so this interval is modified when the substation is hardened, as shown in (4).

$$P_{ts}(a_b=0) \in \left[\bar{P}^{LB}(PGA_{bts}) - K_{bts}^{LB}x_b^H,\ \bar{P}^{UB}(PGA_{bts}) - K_{bts}^{UB}x_b^H\right]. \tag{4}$$

Note that, from (1) it is clear that there are no limitations, in principle, to the type of component that can be hardened. To model hardening decisions for any component (e.g., a generator), $\boldsymbol{x}^H$ must contain a binary decision variable associated with it, and $K_{ts}$ must be selected so as to decrease its failure probability when the corresponding component of $\boldsymbol{x}^H$ equals one. This work focuses on hardening substations, as these have shown to be particularly vulnerable against earthquakes [6]. Furthermore, note that the model can also consider investments in new substations, which only requires to consider transmission line candidates that connect existing substations to the candidate substation. Overall, the model is flexible and portfolios of hardening and expansion measures may be useful to deal with other natural hazards (e.g., windstorms, wildfires, floods).

### C. Mathematical Formulation

*1) Complete Formulation:* In this formulation, both the objective function and constraints are presented in an expanded manner. The complete formulation for the proposed network planning model corresponds to the following three-level optimization problem:

$$\underset{\substack{\Delta D_{bet}^+,\Delta D_{bet}^-,\Delta_{bt}^{FD},\theta_{bt},\\ f_{lt},p_{it},r_{ikt}^d,r_{ikt}^u,x_{it}^{UC},x_l^L,x_b^H}}{\text{Minimize}} \sum_{t\in\mathcal{T}} h_t \Bigg[\sum_{i\in I}\Bigg(C_i^p p_{it} + \sum_{k\in\mathcal{K}}\left(C_{ik}^d r_{ikt}^d + C_{ik}^u r_{ikt}^u\right)\Bigg) + \sum_{b\in N}\Bigg(C_b^{FD}\Delta_{bt}^{FD} + \sum_{e\in\mathcal{E}}\left(C_{be}^{I+}\Delta D_{bet}^+ + C_{be}^{I-}\Delta D_{bet}^-\right)\Bigg) + \sum_{s\in\mathcal{S}}\mathbb{p}_s \sup_{P\in\mathcal{P}_{ts}(\boldsymbol{x}^H)} \mathbb{E}_P\{H_t(\boldsymbol{a}_{ts},\boldsymbol{p},\boldsymbol{r^d},\boldsymbol{r^u},\boldsymbol{\Delta^{FD}},\boldsymbol{\Delta D^+},\boldsymbol{\Delta D^-},\boldsymbol{x}^L)\}\Bigg] + \sum_{l\in\mathcal{L}^C} C_l^L x_l^L + \sum_{b\in N_h} C_b^h x_b^H \tag{5}$$

subject to:

$$\sum_{i\in I_b} p_{it} + \sum_{l\in\mathcal{L}|to(l)=b} f_{lt} - \sum_{l\in\mathcal{L}|fr(l)=b} f_{lt} = D_{bt}; \forall b\in N, t\in\mathcal{T} \tag{6}$$

$$f_{lt} = b_l(\theta_{fr(l),t} - \theta_{to(l),t}); \forall l\in\mathcal{L}^E, t\in\mathcal{T} \tag{7}$$

$$-M(1-x_l^L) + b_l(\theta_{fr(l),t} - \theta_{to(l),t}) \leq f_{lt} \leq b_l(\theta_{fr(l),t} - \theta_{to(l),t}) + M(1-x_l^L); \forall l\in\mathcal{L}^C, t\in\mathcal{T} \tag{8}$$

$$-\overline{F}_l \leq f_{lt} \leq \overline{F}_l; \forall l\in\mathcal{L}^E, t\in\mathcal{T} \tag{9}$$

$$-x_l^L \overline{F}_l \leq f_{lt} \leq x_l^L \overline{F}_l; \forall l \in \mathcal{L}^C, t \in \mathcal{T} \quad (10)$$

$$p_{it} - \sum_{k \in \mathcal{K}} r_{ikt}^d \geq \underline{P}_i x_{it}^{UC}; \forall i \in I, t \in \mathcal{T} \quad (11)$$

$$p_{it} + \sum_{k \in \mathcal{K}} r_{ikt}^u \leq \overline{P}_i x_{it}^{UC}; \forall i \in I, t \in \mathcal{T} \quad (12)$$

$$0 \leq r_{ikt}^d \leq \overline{R}_{ik}^D; \forall i \in I, k \in \mathcal{K}, t \in \mathcal{T} \quad (13)$$

$$0 \leq r_{ikt}^u \leq \overline{R}_{ik}^U; \forall i \in I, k \in \mathcal{K}, t \in \mathcal{T} \quad (14)$$

$$0 \leq \Delta_{bt}^{FD} \leq \overline{\Delta}_b^{FD}; \forall b \in N, t \in \mathcal{T} \quad (15)$$

$$0 \leq \Delta D_{bet}^{+} \leq \overline{\Delta D}_{be}^{+}; \forall b \in N, e \in \mathcal{E}, t \in \mathcal{T} \quad (16)$$

$$0 \leq \Delta D_{bet}^{-} \leq \overline{\Delta D}_{be}^{-}; \forall b \in N, e \in \mathcal{E}, t \in \mathcal{T} \quad (17)$$

$$p_{wt} \leq \zeta_{wt} \overline{P}_i; \forall w \in \mathcal{W}, t \in \mathcal{T} \quad (18)$$

$$x_{it}^{UC} \in \{0,1\}; \forall i \in I, t \in \mathcal{T} \quad (19)$$

$$x_l^L \in \{0,1\}; \forall l \in \mathcal{L}^C \quad (20)$$

$$x_b^H \in \{0,1\}; \forall b \in N_h. \quad (21)$$

In model (5)–(21), $\mathcal{K}$ is the set of indices for the snapshots utilized to discretize post-contingency operation, and $\mathcal{E}$ contains the indices for power imbalance steps (where a step represents an amount of power that can be scheduled at a given unit cost). $\mathcal{L}^E$ and $\mathcal{L}^C$ are subsets of $\mathcal{L}$, which consider only existing and candidate lines, respectively. $\mathcal{T}$ is the set of all time blocks, whereas set $\mathcal{S}$ contains the indices of all scenarios. Sets $\mathcal{W}$ and $I_b$ are subsets of $I$, and contain the indices of renewable generators, and of those generators connected to bus $b$, respectively. $N_h$ is the subset of $N$ containing the indices of substations that can be hardened. Parameters include $\overline{\Delta D}_{be}^{+}$, $\overline{\Delta D}_{be}^{-}$, $\overline{\Delta}_b^{FD}$, which are the maximum net load increase, decrease, and demand shifting, respectively. $\overline{F}_l$ represents the maximum power flow per line (or line capacity), while $\underline{P}_i$ and $\overline{P}_i$ represent minimum and maximum generation capacities. Maximum upward and downward reserves are represented by $\overline{R}_{ik}^U$ and $\overline{R}_{ik}^D$, while $\zeta_{wt}$ is the availability of renewable resources. Nodal demand is $D_{bt}$, $h_t$ is the number of hours represented by each time block, and $b_l$ denotes the susceptance of each line. $M$ is a large constant, the probability of each scenario is represented by $\mathbb{p}_s$, and $H_t$ is the function that computes the minimum cost of corrective actions. Cost coefficients comprise $C_i^p$, $C_{ik}^u$, $C_{ik}^d$, $C_b^{FD}$, $C_{be}^{I+}$, $C_{be}^{I-}$, $C_b^h$, and $C_l^L$, that respectively represent the costs of energy, scheduling of upward reserves, downward reserves, load shifting, net load increase, net load reduction, the costs of hardening substations, and costs of investing in new lines. Finally, decision variables include the scheduled net load increase ($\Delta D_{bet}^{+}$), scheduled net load reduction ($\Delta D_{bet}^{-}$), scheduled load to be shifted ($\Delta_{bt}^{FD}$), voltage angles ($\theta_{bt}$), power flows ($f_{lt}$), power outputs ($p_{it}$), scheduled downward and upward reserves ($r_{ikt}^d$ and $r_{ikt}^u$), commitment of generators ($x_{it}^{UC}$), installation of new lines ($x_l^L$), and substation hardening decisions ($x_b^H$).

The objective function to be minimized is presented in (5). This considers the costs of operation, consisting of the costs of energy and the costs of scheduling post-contingency services provided by generation and demand. It also considers the costs of investment in new assets and in substation hardenings, as well as the worst-case (in terms of probability distribution) expected value of corrective action costs. It is worth noting that the proposed model is probabilistic, and thus considers the cost of each outage weighted by its probability (which may change) and does not optimize against the worst-case contingency only.

Constraint (6) enforces power balance at each bus of the system, noting that there is no demand-side participation since, in this model, DER services are only intended to provide support against contingencies as in [24]. Constraints (7) and (8) model the DC power flows, while constraints (9) and (10) ensure that thermal limits of existing and candidate lines are met. Constraints (11) and (12) ensure that the power of each generator is within its technical limits, even after delivering its reserves. The maximum upward and downward reserves that can be scheduled for every snapshot are limited by constraints (13) and (14), which model the ramping limit of each generator. The maximum available DER to be scheduled on post-contingency services are represented by constraints (15), (16) and (17). Finally, the resource availability of each renewable generator is modeled by constraint (18), while constraints (19), (20), and (21) state that commitment, network investment, and substation hardening are binary decisions.

*2) Operation Under Contingency:* This model determines the minimum-cost corrective actions to perform in case of a contingency. Here, generation and line outages are modeled through two states representing their full availability or unavailability due to faults. Instead, in the case of substations various damage states are considered, representing partial availability of substation capacity after an earthquake occurs. Importantly, when a substation is damaged, the capacities of all equipment connected to it (generators, lines/transformers, and loads) are derated. Next, we describe the operation under contingency model.

$$H_t(\boldsymbol{x}_t, \boldsymbol{a}_{ts}) = \underset{\substack{\Delta_{bk}^{FD+c}, \Delta_{bk}^{FD-c}, \\ \Delta D_{bke}^{+c}, \Delta D_{bke}^{-c}, \\ \theta_{bk}^c, f_{lk}^c, p_{ik}^c, r_{ik}^{dc}, r_{ik}^{uc}}}{\text{Minimize}} \sum_{k \in \mathcal{K}} \Big[ \sum_{i \in I} \left( C_{ik}^{dc} r_{ik}^{dc} + C_{ik}^{uc} r_{ik}^{uc} \right) + \sum_{b \in N, e \in \mathcal{E}} \left( C_{be}^{I+^c} \Delta D_{bke}^{+c} + C_{be}^{I-^c} \Delta D_{bke}^{-c} \right) + \sum_{b \in N} C_b^D LS_{bk} + \sum_{i \in I} C_i^G GS_{ik} \Big] \Delta t + \sum_{b \in N} C_b^{FD^c} \Delta_{b1}^{FD-c} \quad (22)$$

subject to:

$$\sum_{i \in I_b} p_{ik}^c + \sum_{l \in \mathcal{L} | to(l)=b} f_{lk}^c - \sum_{l \in \mathcal{L} | fr(l)=b} f_{lk}^c + \Delta_{bk}^{FD-c} - \Delta_{bk}^{FD+c} + \sum_{e \in \mathcal{E}} \left( \Delta D_{bke}^{-c} - \Delta D_{bke}^{+c} \right) = D_{bt} - LS_{bk}; \forall b \in N, k \in \mathcal{K} \quad (23)$$

$$-a_l^L \overline{F}_l \leq f_{lk}^c \leq a_l^L \overline{F}_l; \forall l \in \mathcal{L}^E, k \in \mathcal{K} \quad (24)$$

$$-a_l^L x_l^L \overline{F}_l \leq f_{lk}^c \leq a_l^L x_l^L \overline{F}_l; \forall l \in \mathcal{L}^C, k \in \mathcal{K} \quad (25)$$

$$-d_{to(l)}^N \overline{F}_l \leq f_{lk}^c \leq d_{to(l)}^N \overline{F}_l; \forall l \in \mathcal{L}^E, k \in \mathcal{K} \quad (26)$$

$$-d_{fr(l)}^N \overline{F}_l \leq f_{lk}^c \leq d_{fr(l)}^N \overline{F}_l; \forall l \in \mathcal{L}^E, k \in \mathcal{K} \quad (27)$$

$$-d^N_{to(l)}x^L_l\overline{F}_l \le f^c_{lk} \le d^N_{to(l)}x^L_l\overline{F}_l; \forall l \in \mathcal{L}^C, k \in \mathcal{K} \quad (28)$$

$$-d^N_{fr(l)}x^L_l\overline{F}_l \le f^c_{lk} \le d^N_{fr(l)}x^L_l\overline{F}_l; \forall l \in \mathcal{L}^C, k \in \mathcal{K} \quad (29)$$

$$-M\left(3-\left(a^L_l + a^{N_{|\mathcal{D}|}}_{fr(l)} + a^{N_{|\mathcal{D}|}}_{to(l)}\right)\right) + b_l\left(\theta^c_{fr(l),k} - \theta^c_{to(l),k}\right) \le f^c_{lk} \le b_l\left(\theta^c_{fr(l),k} - \theta^c_{to(l),k}\right) + M\left(3-\left(a^L_l + a^{N_{|\mathcal{D}|}}_{fr(l)} + a^{N_{|\mathcal{D}|}}_{to(l)}\right)\right); \forall l \in \mathcal{L}^E, k \in \mathcal{K} \quad (30)$$

$$-M\left(3-x^L_l\left(a^L_l + a^{N_{|\mathcal{D}|}}_{fr(l)} + a^{N_{|\mathcal{D}|}}_{to(l)}\right)\right) + b_l\left(\theta^c_{fr(l),k} - \theta^c_{to(l),k}\right) \le f^c_{lk} \le b_l\left(\theta^c_{fr(l),k} - \theta^c_{to(l),k}\right) + M\left(3-x^L_l\left(a^L_l + a^{N_{|\mathcal{D}|}}_{fr(l)} + a^{N_{|\mathcal{D}|}}_{to(l)}\right)\right); \forall l \in \mathcal{L}^C, k \in \mathcal{K} \quad (31)$$

$$p^c_{ik} = p_{it}a^G_{is} + r^{uc}_{ik} - r^{dc}_{ik} - GS_{ik}; \forall i \in I, k \in \mathcal{K} \quad (32)$$

$$p^c_{ik} \le \overline{P}_i d^N_{bus(i)}; \forall i \in I, k \in \mathcal{K} \quad (33)$$

$$0 \le r^{dc}_{ik} \le r^d_{ikt}a^G_i; \forall i \in I, k \in \mathcal{K} \quad (34)$$

$$0 \le r^{uc}_{ik} \le r^u_{ikt}a^G_i; \forall i \in I, k \in \mathcal{K} \quad (35)$$

$$0 \le \Delta D^{+c}_{bke} \le \Delta D^+_{bet}; \forall b \in N, k \in \mathcal{K}, e \in \mathcal{E} \quad (36)$$

$$0 \le \Delta D^{-c}_{bke} \le \Delta D^-_{bet}; \forall b \in N, k \in \mathcal{K}, e \in \mathcal{E} \quad (37)$$

$$0 \le \Delta^{FD-c}_{bk} \le \Delta^{FD}_{bt}; \forall b \in N, k \in \mathcal{K} \quad (38)$$

$$\delta\sum_{k\in\mathcal{K}}\Delta^{FD-c}_{bk} = \sum_{k\in\mathcal{K}}\Delta^{FD+c}_{bk}; \forall b \in N \quad (39)$$

$$\Delta^{FD-c}_{b1} \ge \Delta^{FD-c}_{bk}; \forall b \in N, k \in \mathcal{K}\setminus\{1\} \quad (40)$$

$$\Delta D^{+c}_{b1e} \ge \Delta D^{+c}_{bke}; \forall b \in N, k \in \mathcal{K}\setminus\{1\}, e \in \mathcal{E} \quad (41)$$

$$\Delta D^{-c}_{b1e} \ge \Delta D^{-c}_{bke}; \forall b \in N, k \in \mathcal{K}\setminus\{1\}, e \in \mathcal{E} \quad (42)$$

$$D_{bt} - LS_{bk} - \sum_{e\in\mathcal{E}}\left(\Delta D^{-c}_{bke} - \Delta D^{+c}_{bke}\right) - \Delta^{FD-c}_{bk} + \Delta^{FD+c}_{bk} \le \overline{D}_b d^N_b; \forall b \in N, k \in \mathcal{K}, \quad (43)$$

In this model, coefficients $C^{dc}_{ik}, C^{uc}_{ik}, C^{I+^c}_{be}, C^{I-^c}_{be}, C^{FD^c}_b$, represent, respectively, the utilization costs of downward reserves, upward reserves, net load increase, net load reduction, and demand shifting, whereas coefficients $C^D_b$ and $C^G_i$ represent the cost of demand shedding and generation curtailment. Additionally, $\overline{D}_b$ represents the maximum demand of the substation, $\Delta t$ is the total duration of each post-contingency snapshot $k$, and $\delta$ models the energy payback from demand shifting (where the payback represents the extra energy demanded in future snapshots due to deferring energy consumptions). The variables are voltage angles ($\theta^c_{bk}$), power flows ($f^c_{lk}$), generation curtailment ($GS_{ik}$), load shedding ($LS_{bk}$), power outputs ($p^c_{ik}$), downward and upward reserves utilization ($r^{dc}_{ik}$ and $r^{uc}_{ik}$), positive and negative deviations from nominal demand due to demand shifting ($\Delta^{FD+c}_{bk}$ and $\Delta^{FD-c}_{bk}$), net load increase ($\Delta D^{+c}_{bke}$), and net load reduction ($\Delta D^{-c}_{bke}$).

As stated in (22), the objective function considers the costs of load shedding, generation curtailment, and the utilization costs of post-contingency services from generators (reserves) and DER. The total cost of the load shifting service depends on the magnitude of the first (and also the largest) disconnection, whereas the cost of the other two DER services depends on the total energy injected or withdrawn.

Nodal power balance is enforced by (23), which considers the utilization of voluntary and involuntary corrective actions. Constraints (24) and (25) limit the maximum power flows, considering that lines may be outaged or not built. Maximum capacity of lines can also be reduced by outages on their terminal substations, which is expressed by constraints (26), (27), (28) and (29). Also, DC power flow equations are utilized, as stated by constraints (30) and (31).

The post-contingency power outputs depend on their pre-contingency value, the utilization of reserves, and power curtailment as stated by constraint (32). Additionally, the maximum power injected by generators can be limited due to potential damage in substations, which is expressed by (33). Constraints (34) and (35) limit the maximum amount of reserves to be delivered, while constraints (36), (37) and (38) limit the utilization of DER services by the amount scheduled pre-contingency. Constraint (39) ensures power balance on loads providing the demand shift service, while constraint (40) ensures that the demand that will be shifted is disconnected immediately after the contingency. For the other DER services, constraints (41) and (42) enforce that the first load reduction/increase is the largest one. The maximum amount of power withdrawn by loads, given the damage state of the substation, is modeled by constraint (43).

### D. Reducing Model Complexity

In order to properly determine cost-effective network enhancements to increase resilience, the proposed model captures a number of details about the system before and during contingencies. These details are usually modeled within the existing resilient planning literature, and include DC power flows [13], [17], utilizing several operating conditions to capture the impacts of hazards on the system [22], considering several contingency scenarios for each hazard [9], [16], and modeling the operation under contingency through several time-coupled snapshots [1], [12]. These characteristics add complexity to the mathematical model, increasing the computational burden for its solution. However, a series of simplifications can be conducted to decrease this burden. Firstly, system operation can be represented by the most stressed conditions, thus requiring a few time blocks. Additionally, the analysis for network enhancements can be carried out by zone, reducing the number of earthquakes that need to be modeled. Finally, as explained in previous sections, the user can choose the set of contingencies to be considered (by properly selecting the set $\mathcal{A}$), thus being able to give more resolution to areas near each earthquake in terms of modeling multiple outages.

## III. Solution Methodology

### A. Compact Formulation

The compact formulation corresponds to the problem (5)–(21) whereby variables and constraints are grouped, making mathematical manipulations simpler. This formulation is presented in

the following optimization program:

$$\underset{\boldsymbol{x}_t \in \mathcal{X}_t}{\text{Minimize}} \sum_{t\in\mathcal{T}} h_t \Bigg[ \boldsymbol{c}^{Op^T} \boldsymbol{x}_t^{Op} + \boldsymbol{c}^{UC^T} \boldsymbol{x}_t^{UC} + \sum_{s\in\mathcal{S}} \mathbb{p}_s \cdot \sup_{P\in\mathcal{P}_{ts}(\boldsymbol{x}^H)} H_t(\boldsymbol{x}_t, \boldsymbol{a}_{ts}) \Bigg] + \boldsymbol{c}^{L^T} \boldsymbol{x}^L + \boldsymbol{c}^{H^T} \boldsymbol{x}^H \quad (44)$$

subject to:

$$A\boldsymbol{x}_t \leq \boldsymbol{q}_t, \forall t \in \mathcal{T}, \quad (45)$$

where $\boldsymbol{x}_t = [\boldsymbol{x}_t^{Op}, \boldsymbol{x}_t^{UC}, \boldsymbol{x}^L, \boldsymbol{x}^H]$. The objective function (44) corresponds to (5), whereas (45) represents constraints (6)–(18). Finally, the set $\mathcal{X}_t$ comprises the feasible points for the binary variables defined by (19)–(21).

Similarly, next we present a compact formulation of problem (22)–(43):

$$H_t(\boldsymbol{x}_t, \boldsymbol{a}_{ts}) = \underset{\boldsymbol{y}}{\text{Minimize}}\ v_t^T \boldsymbol{y}_t \quad (46)$$

subject to:

$$B_t \boldsymbol{y}_t \geq e_t : (\Theta_t) \quad (47)$$

$$C_t \boldsymbol{y}_t \geq D_t \boldsymbol{x}_t + g_t : (\Phi_t) \quad (48)$$

$$G_t \boldsymbol{y}_t \geq J_t(\boldsymbol{a}_{ts}) \boldsymbol{x}_t + w_t : (\Lambda_t) \quad (49)$$

$$L_t \boldsymbol{y}_t \geq u_t(\boldsymbol{a}_{ts}) : (\Gamma_t), \quad (50)$$

where the objective function (46) corresponds to (22). Constraint (47) groups constraints (23) and (39)–(42). Similarly, (48) is associated with (36)–(38). Constraint (49) corresponds to (25), (28), (29), (31), (32), (34) and (35). Finally, (50) represents constraints (24), (26), (27), (30), (33), and (43).

### *B. Problem Reformulation and Solution Algorithm*

We can reformulate the compact model (44)–(45) by expanding the worst-case expected costs of corrective actions, thereby obtaining model (51)–(55). In this reformulation, the inner problem maximizes the expected cost of contingencies expressed by (53), where (54) makes sure that the (decision-dependent) probability distribution is within the set of candidate distributions (which was presented in (1)). Note that the summation of all probabilities is equal to one, as guaranteed by (55).

$$\underset{\alpha_{ts}, \boldsymbol{x}_t \in \mathcal{X}_t}{\text{Minimize}} \sum_{t\in T} h_t \Big[ \boldsymbol{c}^{Op^T} \boldsymbol{x}_t^{Op} + \boldsymbol{c}^{UC^T} \boldsymbol{x}_t^{UC} \Big] + \boldsymbol{c}^{L^T} \boldsymbol{x}^L + \boldsymbol{c}^{H^T} \boldsymbol{x}^H + \sum_{t\in T} h_t \sum_{s\in\mathcal{S}} \mathbb{p}_s \alpha_{ts} \quad (51)$$

subject to:

$$A\boldsymbol{x}_t \leq \boldsymbol{q}_t, \forall t \in \mathcal{T} \quad (52)$$

$$\alpha_{ts} = \Big\{ \underset{P}{\text{Maximize}} \sum_{a_{ts}\in\mathcal{A}} H_t\big(\boldsymbol{x}_t, \boldsymbol{a}_{ts}\big) P(\boldsymbol{a}_{ts}) \quad (53)$$

subject to:

$$\sum_{a_{ts}\in\mathcal{A}} S_{ts} \boldsymbol{a}_{ts} P(\boldsymbol{a}_{ts}) \leq \overline{\boldsymbol{\mu}}_{ts} + K_{ts} \boldsymbol{x}^H : (\boldsymbol{\pi}_{ts}) \quad (54)$$

$$\sum_{a_{ts}\in\mathcal{A}} P(\boldsymbol{a}_{ts}) = 1 : (\varphi_{ts}) \Big\}, \forall t \in \mathcal{T}, s \in \mathcal{S}_t. \quad (55)$$

TABLE I
CANDIDATE TRANSMISSION LINES

| Line ID | Type | Capacity [MW] | Bus From | Bus To | Length [km] | Cost [million$/yr] |
|---|---|---|---|---|---|---|
| L1 | DC | 2x750 | 4 | 29 | 1239 | 212 |
| L2 | AC | 2x375 | 37 | 40 | 97 | 3.0 |
| L3 | AC | 2x375 | 8 | 9 | 210 | 7.9 |
| L4 | AC | 2x250 | 33 | 37 | 352 | 8.8 |
| L5 | AC | 2x375 | 25 | 30 | 99 | 3.7 |

TABLE II
CANDIDATE SUBSTATION HARDENINGS

| Substation ID | Substation number | Cost [million$/yr] |
|---|---|---|
| S1 | 30 | 3.9 |
| S2 | 29 | 3.9 |
| S3 | 34 | 3.9 |
| S4 | 6 | 3.9 |
| S5 | 26 | 3.9 |

By replacing the inner maximization problem by its dual, we obtain a two-level optimization program. The products between continuous and binary variables are linearized through additional constraints as in [32]. The problem is solved until a 0.05%-global optimality through the classical (exact) column-and-constraint-generation algorithm ([31] and [24]). For the interested reader, the decomposition and solution algorithm can be found in the on-line appendix [33].

## IV. CHILEAN SYSTEM CASE STUDY

This case study seeks to illustrate the proposed model as well as identify and discuss the optimal investment decisions in the Chilean power network that serve to hedge risks associated with earthquakes. The power network modeled corresponds to a simplified 40-bus representation of the Chilean system by 2024, which is presented in Fig. 3. This network contains 110 transmission assets, 11.9 GW of peak demand, and 30 GW of generation installed capacity distributed among 226 generating units, dominated by hydro (25%), coal (16%), LNG (8%), and combined participation of wind and solar power generation (30%). Specific costs, capacities and other system data are obtained from [34], including new generation and transmission projects which allow us to update the system for the projected state in 2024. Four major double circuit lines are considered in this analysis as candidate investments, plus an HVDC link connecting the north of the country with the main load center in Santiago. This HVDC link has been proposed primarily to transfer renewable energy from the Atacama desert, a prominent area for new solar power projects as explained in [35]. The most important characteristics of these candidate lines are presented in Table I. Additionally, Table II presents five substations that can be hardened in order to make them more robust against earthquakes. Finally, demand on the two biggest cities of the country (i.e., Santiago and Concepcion) can provide the three DER services proposed.

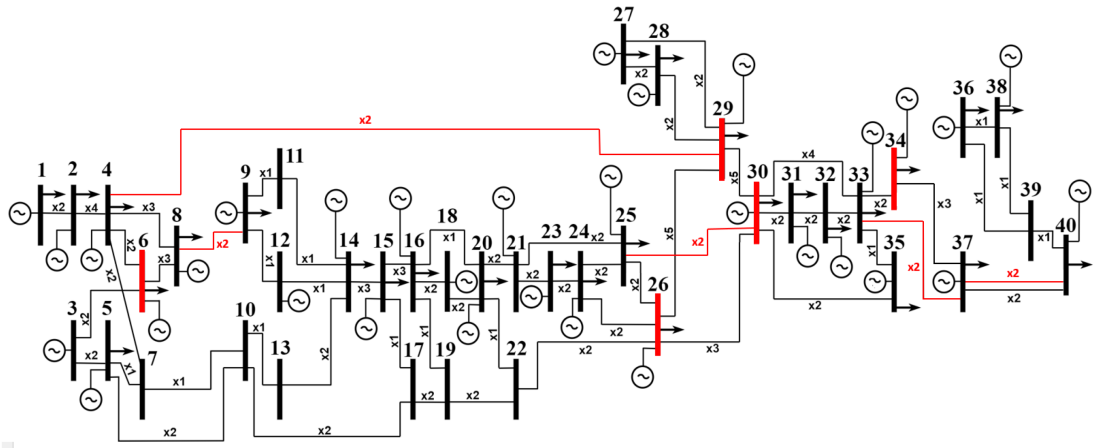

Fig. 3. Chilean transmission network used in the case studies, indicating number of circuits per link. Candidate transmission lines and substations are marked in red.

Also, we model 4 scenarios: a first scenario representing normal conditions without earthquakes; a second scenario with an earthquake occurring in northern Chile, particularly in the city of Antofagasta; a third scenario with an earthquake occurring in central Chile, particularly in the city of Santiago; and a fourth scenario with an earthquake occurring in southern Chile, particularly in the city of Concepcion. Earthquakes modeled are of magnitude 7.5Mw with 50-km depth hypocenter. The PGA spatial profile produced by these hazards follows [29]. Through the fragility curves developed in [7], [30], earthquakes increase outage probabilities, potentially originating outages of generators, outages of transmission lines, and outages of substations that can feature two levels of damage (with 70% and 100% capacity degradation). For the scenario without earthquakes, we use the reliability data published by the Chilean system operator (SO) and available in [36] to calculate failure rates of network components under normal conditions.

In order to model the most stressed operating condition, yearly operation is represented by one peak-demand time block. Post-contingency operation is discretized utilizing two time-coupled snapshots of 30 minutes each. For the scenario without earthquakes, only single outages are considered, whereas for earthquake scenarios we include single outages and double outages. To reduce the number of double outages, we consider only failure on the components that are most affected by the hazard, specifically, those connected to the five substations nearest to the earthquake's epicenter.

The model is implemented in Julia JuMP [37], and solved with Gurobi 9.0 on a server with 10 CPUs and 32 GB of RAM.

### A. Results and Analysis

In this section we analyze six case studies that are presented in Table III. The earthquake probability corresponds to the sum of the probabilities of earthquake scenarios 2, 3 and 4 (note scenario 1 represents a normal condition without earthquake occurrence).

Table IV presents the results of the six case studies when the network is optimally enhanced (upper row of each cost component) and when the network is not enhanced at all (lower row of each cost component). This table shows the costs associated with the optimal operation and investment decisions (when applicable), as well as an estimation of the expected cost of corrective actions. The latter is computed by carrying out 400,000 Monte Carlo simulations of outages (100,000 simulations per earthquake scenario, including the one without earthquakes), considering the appropriate conditional probabilities (which depend on hardening decisions in the case of substations).

The upper rows of the cost components in Table IV show that the network is enhanced in order to hedge the system against

TABLE III
CASE STUDIES

| | Case 1 | Case 2 | Case 3 | Case 4 | Case 5 | Case 6 |
|---|---|---|---|---|---|---|
| Earthquake probability | 0.25% | 0.50% | 0.75% | 1.00% | 1.25% | 2.50% |

TABLE IV
COSTS (IN MILLION$/YR) FOR EACH CASE, WITH (UPPER ROW OF EACH COST COMPONENT) AND WITHOUT NETWORK ENHANCEMENTS (LOWER ROW OF EACH COST COMPONENT)

| | Case 1 | Case 2 | Case 3 | Case 4 | Case 5 | Case 6 |
|---|---|---|---|---|---|---|
| Energy generation | 1138.4 | 1138.4 | 1138.4 | 1138.4 | 1138.4 | 1138.4 |
| | 1138.4 | 1138.4 | 1138.4 | 1138.4 | 1138.4 | 1165.0 |
| Reserves | 24.6 | 25.1 | 25.5 | 25.5 | 26.8 | 25.5 |
| | 24.6 | 25.5 | 28.9 | 28.9 | 28.9 | 47.5 |
| DER | 8.7 | 8.7 | 8.7 | 8.7 | 8.7 | 8.7 |
| | 8.7 | 8.7 | 8.7 | 8.7 | 8.7 | 8.7 |
| New lines | 0.0 | 0.0 | 0.0 | 8.8 | 8.8 | 8.8 |
| | - | - | - | - | - | - |
| Hardening | 7.9 | 15.8 | 15.8 | 15.8 | 19.7 | 19.7 |
| | - | - | - | - | - | - |
| Corrective actions | 83.3 | 95.1 | 110.7 | 136.7 | 138.1 | 220.8 |
| | 98.2 | 127.7 | 157.4 | 189.1 | 221.8 | 332.4 |
| **Total** | **1262.9** | **1283.1** | **1299.1** | **1333.9** | **1340.5** | **1421.9** |
| | **1269.9** | **1300.3** | **1333.4** | **1365.1** | **1397.8** | **1553.6** |

TABLE V
RELIABILITY METRICS FOR EACH CASE, WITH (UPPER ROW OF EACH METRIC) AND WITHOUT NETWORK ENHANCEMENTS (LOWER ROW OF EACH METRIC)

| | Case 1 | Case 2 | Case 3 | Case 4 | Case 5 | Case 6 |
|---|---|---|---|---|---|---|
| EENS | 0.97 | 1.36 | 1.91 | 2.57 | 2.96 | 5.76 |
| [GWh] | 1.48 | 2.60 | 3.81 | 5.09 | 6.37 | 11.41 |
| $CVaR_{95\%}$ | 10.84 | 15.35 | 20.92 | 28.13 | 31.31 | 59.91 |
| ENS [GWh] | 13.40 | 20.22 | 28.98 | 38.35 | 47.86 | 86.00 |
| LOLE | 8.33 | 3.78 | 5.27 | 6.47 | 7.24 | 12.73 |
| [hr] | 9.82 | 5.77 | 7.59 | 9.84 | 12.36 | 19.91 |

TABLE VI
OPTIMAL NETWORK ENHANCEMENTS WHEN SUBSTATION HARDENING IS (ROWS 1&3) AND IS NOT (ROWS 2&4) CONSIDERED

| | Case 1 | Case 2 | Case 3 | Case 4 | Case 5 | Case 6 |
|---|---|---|---|---|---|---|
| New lines | - | - | - | L4 | L4 | L4 |
| | - | - | - | L4 | L4 | L1,L4 |
| Hardened subs. | S3-S4 | S2-S5 | S2-S5 | S2-S5 | S1-S5 | S1-S5 |
| | - | - | - | - | - | - |

the possibility of undergoing an earthquake. Furthermore, when these events are deemed as more likely, a more robust network is needed, which shows the relevance of properly assessing the seismic risk at the transmission expansion planning stage. Interestingly, cases 1–3 only invest in hardening options, while cases 4–6 also invest in new lines. This demonstrates that there is a preference towards hardening options to hedge against earthquakes since lines are only installed once almost all candidate substations have been hardened (4 out of 5 substations in case 4). The above decisions are combined with the utilization of DER services located in the demand centers, particularly the net load reduction service that is utilized to its maximum availability in all cases (262 MW, corresponding to 5% of the demand of the substations that provide the service), whereas load increase and demand shifting services are not required. Note that the net load reduction service (through distributed generation, for instance) is particularly attractive to secure supply against earthquakes, as it can decrease load curtailments without the need for resilience provision from the main grid.

Additionally, Table IV shows that the total cost of the system increases when the network cannot be enhanced. This is particularly clear when the probability of earthquakes is higher. The difference between the results with and without network enhancements is mainly justified by the higher expected cost of corrective actions when there are no network enhancements. Also, in some cases, when the network is not enhanced, the system requires more operation-level resources to increase the security of supply (e.g., higher volumes of generation reserves).

In order to analyze the reliability of the system in each case, we utilized the results of the Monte Carlo simulations to compute three reliability metrics that are shown in Table V. The first metric corresponds to the expected value of energy not supplied (EENS). The second metric is the conditional value at risk (CVaR) at the 95%, which is computed as the average energy not supplied in the worst 5% of scenarios. Finally, the third metric corresponds to the loss of load expectation, which is equal to the expected number of hours with unsupplied demand over a year. Expectedly, when the probability of earthquakes increases, the reliability of the system decreases, as shown by the increased energy not supplied, both in expected value and in the worst scenarios. Additionally, the results show that network enhancements provide benefits in terms of increased reliability too (beyond the resilience benefits reflected by the decrease in $CVaR_{95\%}$), as demonstrated by the improved reliability metrics when compared to the case in which enhancements are not considered.

Rows 1 and 3 of Table VI show optimal investments when hardening is considered by the model. Rows 2 and 4 show optimal investments when hardening is neglected. Interestingly, there is no investment in cases 1-3 when hardening options are not allowed, demonstrating that new lines do not significantly contribute to improve system resilience in these cases. Remarkably, at least 4 candidate substations (namely, S2 to S5) are selected in almost all the cases, beside case 1, demonstrating, again, that substation hardening is a valuable choice to hedge against earthquakes. Although lines are less attractive than substation hardenings, it is important to highlight that the new lines selected to be installed, namely lines L1 and L4, feature special topological characteristics to boost resilience. For example, L1 corresponds to an HVDC link with more than 1000 km. This line connects directly, in a point-to-point fashion, production centre in the north (where high penetration of solar power generation is located) with the main load center in Santiago, bypassing all substations in the main transmission corridor between the north and the center of the country/network. This topological characteristic is key since it adds a new route to transfer power between two critical points of the network. Additionally, this new link avoids substations in-between that are prone to present some level of damage right after an earthquake occurs. Note that when substation hardenings are not considered, the system may need more investment in new assets to attain optimal resilience levels, as shown by case 6. This shows that the need for new transmission infrastructure can be overestimated if hardenings are ignored, highlighting the benefits of considering, simultaneously, these resilience enhancing alternatives within planning models.

### B. Impact of Imprecise Failure Probabilities

This section analyzes the impact that imprecise failure probabilities have on the need for network enhancements. To do so, we determine the optimal portfolio of such enhancements for the same 6 cases of earthquake probabilities while considering three levels of inaccuracy in fragility data. The first level ($\pm 0\%$) contains those cases analyzed in the previous section, where we assumed that outages probabilities are fully accurate, whereas the other two levels feature imprecisions of $\pm 10\%$ and $\pm 30\%$ in PGA. The number of enhancements of the optimal plan in these cases is presented in Fig. 4. Notice that for the same earthquake probability (i.e., the same case), when we consider more inaccurate data, the model decides to invest in

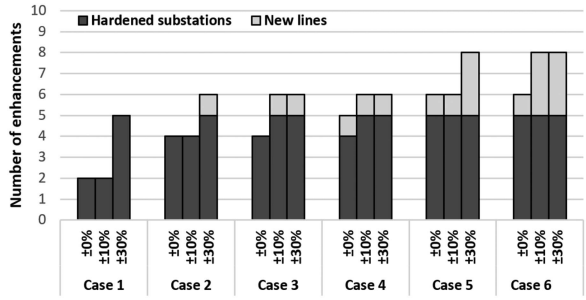


Fig. 4. Optimal number of network enhancements for different levels of uncertainty in fragility data.

TABLE VII
INVESTMENT RESULTS FOR DIFFERENT EARTHQUAKE MAGNITUDES

| | Case 1 | Case 2 | Case 3 |
|---|---|---|---|
| Earthquake magnitude (Mw) | 8.6 | 8.7 | 8.8 |
| Number of hardened substations | 0 | 2 | 2 |
| Number of new lines | 1 | 1 | 1 |

more network enhancements, both hardenings and new lines, in order to attain cost-effective resilience levels. This shows that network enhancements also hedge the system against the uncertainty related to failure likelihoods derived from fragility curves, requiring further investment when these curves are less reliable.

## V. IEEE 118-BUSBAR SYSTEM CASE STUDY

The objective of this section is twofold, firstly, to demonstrate the scalability of the proposed network enhancement model with decision-dependent probabilities and, secondly, to study the impact of the earthquake magnitude on the optimal portfolio of enhancements. To do so, we analyze a case study in the IEEE 118-busbar system, which contains 186 branches, 91 loads, and 54 thermal units. Data for this case study can be found in [38]. In order to compute the impact of earthquakes on the system, we circumscribe the network within a square of side 500 km, assigning a specific location to every component. Additionally, we consider three earthquake scenarios (along with the non-earthquake scenario), with a probability of 0.19% each.

We consider generation reserves and DER services provided at the three busbars with the highest demand as operational measures. Additionally, we consider 5 candidate substations to harden and 6 candidate AC transmission lines. Table VII presents the portfolio of optimal network enhancements. Interestingly, the optimal investment portfolio changes when the earthquakes' magnitude increases. In fact, more investments in substation hardenings are driven by higher earthquake magnitudes, which further emphasizes that substation hardenings are vital for improving the system's resilience against earthquakes.

## VI. CONCLUSION

We propose a model that finds the optimal portfolio of resilient network investments, considering decision-dependent probabilities of outage scenarios. The proposed model can appropriately co-optimize investment choices between installing new network assets and hardening existing network assets, which reduces outage probabilities. The model also balances costs and benefits of proposed investments, which is key to appropriately justify cost-effective and resilient investment propositions. Additionally, the model can also recognize the uncertainty associated with probability values derived from fragility curves by using a distributionally robust optimization approach and also the role played by DER in network investment deferrals. To our knowledge, this is the first model that can carry out the abovementioned assessment in an analytical closed-form fashion. By using our model, we demonstrate the importance of substation hardening decisions to enhance network resilience against earthquakes, combining them with DER services and installation of new network assets. Additionally, our numerical studies suggest that the most attractive candidate lines are those that provide a totally new, alternative path for power, bypassing substations that may suffer outages due to earthquakes. Finally, we demonstrate how resilient investment portfolios can serve to hedge against inaccurate fragility data, highlighting the need to recognize this source of uncertainty and reduce it through better fragility models.

Adapting the model to study how to expand and harden network components to hedge the system against other natural hazards is recommended for future work. For example, it would be interesting to analyze how to hedge the system against windstorms by hardening (e.g., undergrounding) and expanding lines. Optimizing portfolios of hardening and expansion measures can also hedge the system against further natural hazards (e.g., wildfires, floods). In addition, considering line switching as a post-contingency measure in the context of this work is suggested for further studies. Finally, although the main purpose of the proposed model is to determine network enhancements against natural hazards that occur randomly, it can also tackle the problem of securing the system against man-made attacks that are thoroughly decided by the attacker (rather than randomly generated). Note that by setting the correct probability intervals as input data (between 0 and 1; set by $\overline{\boldsymbol{\mu}}_{ts}$ in (1)), our model becomes a fully robust tri-level min-max-min problem (defender-attacker-defender), providing the capability to study terrorist attacks and thus hedging against them through a portfolio of hardening and expansion measures. This is also proposed to be addressed in further research efforts.

## REFERENCES

[1] T. Lagos *et al.*, "Identifying optimal portfolios of resilient network investments against natural hazards, with applications to earthquakes," *IEEE Trans. Power Syst.*, vol. 35, no. 2, pp. 1411–1421, Mar. 2020.
[2] M. Panteli and P. Mancarella, "The grid: Stronger, bigger, smarter?: Presenting a conceptual framework of power system resilience," *IEEE Power Energy Mag.*, vol. 13, no. 3, pp. 58–66, May/Jun. 2015.
[3] Z. Bie, Y. Lin, G. Li, and F. Li, "Battling the extreme: A study on the power system resilience," *Proc. IEEE*, vol. 105, no. 7, pp. 1253–1266, Jul. 2017.
[4] N. Abi-Samra and W. Henry, "Actions before... and after a flood," *IEEE Power Energy Mag.*, vol. 9, no. 2, pp. 52–58, Mar.–Apr. 2011.

[5] B. L. Preston *et al.*, "Resilience of the U.S. electricity system: A multi-hazard perspective," U.S. Department of Energy's Office of Energy Policy and Systems Analysis, Tech. Rep., 2016.
[6] J. C. Araneda, H. Rudnick, S. Mocarquer, and P. Miquel, "Lessons from the 2010 chilean earthquake and its impact on electricity supply," in *Proc. Int. Conf. Power Syst. Technol.*, 2010, pp. 1–7.
[7] Federal Emergency Management Agency, "HAZUS-MH multi-hazard loss estimation methodology, earthquake modeltechnical manual," Washington, DC, USA: Department of Homeland Security.
[8] T. Rossetto, D. D'Ayala, I. Ioannou, and A. Meslem, *Evaluation of Existing Fragility Curves*. Berlin, Germany: Springer, 2014, pp. 47–93.
[9] Y. Tan, A. K. Das, P. Arabshahi, and D. S. Kirschen, "Distribution systems hardening against natural disasters," *IEEE Trans. Power Syst.*, vol. 33, no. 6, pp. 6849–6860, Nov. 2018.
[10] C. He, C. Dai, L. Wu, and T. Liu, "Robust network hardening strategy for enhancing resilience of integrated electricity and natural gas distribution systems against natural disasters," *IEEE Trans. Power Syst.*, vol. 33, no. 5, pp. 5787–5798, Sep. 2018.
[11] W. Yuan, J. Wang, F. Qiu, C. Chen, C. Kang, and B. Zeng, "Robust optimization-based resilient distribution network planning against natural disasters," *IEEE Trans. Smart Grid*, vol. 7, no. 6, pp. 2817–2826, Nov. 2016.
[12] S. Ma, B. Chen, and Z. Wang, "Resilience enhancement strategy for distribution systems under extreme weather events," *IEEE Trans. Smart Grid*, vol. 9, no. 2, pp. 1442–1451, Mar. 2018.
[13] N. R. Romero, L. K. Nozick, I. D. Dobson, N. Xu, and D. A. Jones, "Transmission and generation expansion to mitigate seismic risk," *IEEE Trans. Power Syst.*, vol. 28, no. 4, pp. 3692–3701, Nov. 2013.
[14] S. Ma, L. Su, Z. Wang, F. Qiu, and G. Guo, "Resilience enhancement of distribution grids against extreme weather events," *IEEE Trans. Power Syst.*, vol. 33, no. 5, pp. 4842–4853, Sep. 2018.
[15] S. Ma, S. Li, Z. Wang, and F. Qiu, "Resilience-oriented design of distribution systems," *IEEE Trans. Power Syst.*, vol. 34, no. 4, pp. 2880–2891, Jul. 2019.
[16] J. Yan, B. Hu, K. Xie, J. Tang, and H. Tai, "Data-driven transmission defense planning against extreme weather events," *IEEE Trans. Smart Grid*, vol. 11, no. 3, pp. 2257–2270, May 2020.
[17] R. P. Liu, S. Lei, C. Peng, W. Sun, and Y. Hou, "Data-based resilience enhancement strategies for electric-gas systems against sequential extreme weather events," *IEEE Trans. Smart Grid*, vol. 11, no. 6, pp. 5383–5395, Nov. 2020.
[18] N. Romero, N. Xu, L. K. Nozick, I. Dobson, and D. Jones, "Investment planning for electric power systems under terrorist threat," *IEEE Trans. Power Syst.*, vol. 27, no. 1, pp. 108–116, Feb. 2012.
[19] W. Yuan, L. Zhao, and B. Zeng, "Optimal power grid protection through a defender-attacker-defender model," *Rel. Eng. Syst. Saf.*, vol. 121, pp. 83–89, 2014.
[20] X. Wang, Z. Li, M. Shahidehpour, and C. Jiang, "Robust line hardening strategies for improving the resilience of distribution systems with variable renewable resources," *IEEE Trans. Sustain. Energy*, vol. 10, no. 1, pp. 386–395, Jan. 2019.
[21] C. Shao, M. Shahidehpour, X. Wang, X. Wang, and B. Wang, "Integrated planning of electricity and natural gas transportation systems for enhancing the power grid resilience," *IEEE Trans. Power Syst.*, vol. 32, no. 6, pp. 4418–4429, Nov. 2017.
[22] A. Bagheri, C. Zhao, F. Qiu, and J. Wang, "Resilient transmission hardening planning in a high renewable penetration ERA," *IEEE Trans. Power Syst.*, vol. 34, no. 2, pp. 873–882, Mar. 2019.
[23] R. Moreno *et al.*, "From reliability to resilience: Planning the grid against the extremes," *IEEE Power Energy Mag.*, vol. 18, no. 4, pp. 41–53, Jul./Aug. 2020.
[24] D. Alvarado, A. Moreira, R. Moreno, and G. Strbac, "Transmission network investment with distributed energy resources and distributionally robust security," *IEEE Trans. Power Syst.*, vol. 34, no. 6, pp. 5157–5168, Nov. 2019.
[25] Y. Zhou, M. Panteli, R. Moreno, and P. Mancarella, "System-level assessment of reliability and resilience provision from microgrids," *Appl. Energy*, vol. 230, pp. 374–392, 2018.
[26] J. Cao, W. Du, and H. F. Wang, "An improved corrective security constrained OPF with distributed energy storage," *IEEE Trans. Power Syst.*, vol. 31, no. 2, pp. 1537–1545, Mar. 2016.
[27] Y. Wen, C. Guo, D. S. Kirschen, and S. Dong, "Enhanced security-constrained OPF with distributed battery energy storage," *IEEE Trans. Power Syst.*, vol. 30, no. 1, pp. 98–108, Jan. 2015.
[28] D. F. Recalde Melo, A. Trippe, H. B. Gooi, and T. Massier, "Robust electric vehicle aggregation for ancillary service provision considering battery aging," *IEEE Trans. Smart Grid*, vol. 9, no. 3, pp. 1728–1738, May 2018.
[29] R. Boroschek and V. Contreras, "Strong ground motion from the 2010 mw 8.8 Maule Chile earthquake and attenuation relations for chilean subduction zone interface earthquakes," in *Proc. Int. Symp. Eng. Lessons Learned 2011 Great East Japan Earthquake*, Mar. 2012, pp. 1722–1733.
[30] L. Xie, H. T. Jue Tang, Q. Xie, and S. Xue, "Seismic fragility assessment of transmission towers via performance-based analysis," in *Proc. 15th World Conf. Earthq. Eng.*, 2012.
[31] C. Zhao and R. Jiang, "Distributionally robust contingency-constrained unit commitment," *IEEE Trans. Power Syst.*, vol. 33, no. 1, pp. 94–102, Jan. 2018.
[32] C. C. Petersen, "A note on transforming the product of variables to linear form in linear programs," 1971, working paper, Purdue University.
[33] D. Alvarado, R. Moreno, A. Street, M. Panteli, P. Mancarella, and G. Strbac, "A decision-dependent probability model for planning resilient network investments – auxiliary document," [Online]. Available: https://bit.ly/32Y7lIh
[34] Ministry of Energy Chilean Government, "Proceso de Planificación Energética de Largo Plazo," 2018.
[35] R. Moreno, R. Ferreira, L. Barroso, H. Rudnick, and E. Pereira, "Facilitating the integration of renewables in latin America: The role of hydropower generation and other energy storage technologies," *IEEE Power Energy Mag.*, vol. 15, no. 5, pp. 68–80, Sep. 2017.
[36] Coordinador Eléctrico Nacional, "Informe Preliminar, Estudio de Continuidad de Suministro," 2016.
[37] I. Dunning, J. Huchette, and M. Lubin, "Jump: A modeling language for mathematical optimization," *SIAM Rev.*, vol. 59, no. 2, pp. 295–320, 2017.
[38] A. R. Al-Roomi, "Power flow test systems repository," Halifax, Nova Scotia, Canada, 2015. [Online]. Available: https://al-roomi.org/power-flow